Production of CH ($A^2\Delta$) by multi-photon dissociation of $(CH_3)_2CO$, CH_3NO_2, CH_2Br_2, and $CHBr_3$ at 213 nm*

Li Sheng-Qiang(李胜强), Xu Liang(许 亮), Chen Yang-Qin(陈扬骎), Deng Lian-Zhong(邓联忠), and Yin Jian-Ping(印建平)†

State Key Laboratory of Precision Spectroscopy, Department of Physics, East China Normal University, Shanghai 200062, *China*

(Received 29 December 2013; revised manuscript received 21 February 2014; published online 10 June 2014)

In order to realize electrostatic Stark deceleration of CH radicals and study cold chemistry, the fifth harmonic of a YAG laser is used to prepare CH ($A^2\Delta$) molecules through using the multi-photon dissociation of $(CH_3)_2CO$, CH_3NO_2, CH_2Br_2, and $CHBr_3$ at $\sim$ 213 nm. The CH product intensity is measured by using the emission spectrum of CH ($A^2\Delta \rightarrow X^2\Pi$). The dependence of fluorescence intensity on laser power is studied, and the probable dissociation channels are analyzed. The relationship between the fluorescence intensity and some parameters, such as the temperature of the beam source, stagnation pressure, and the time delay between the opening of pulse valve and the photolysis laser, are also studied. The influence of three different carrier gases on CH signal intensity is investigated. The vibrational and rotational temperatures of the CH ($A^2\Delta$) product are obtained by comparing experimental data with the simulated ones from the LIFBASE program.

Keywords: fifth harmonic of YAG laser, photodissociation, emission spectrum

PACS: 37.10.Pq, 37.10.Mn, 37.10.Vz, 37.20.+j **DOI:** 10.1088/1674-1056/23/8/083701

1. Introduction

Methylidyne radical (CH) is the simplest but a very important hydrocarbon. Its discovery in the laboratory can be traced back to the year 1918.[1,2] Due to its active characteristics, CH radical is beneficial to research in a broad range, such as cold collisions,[3] chemical reaction,[4–8] and the measurement of fundamental constants.[9] CH radical can be produced by many methods, such as chemical reaction,[8,10] photodissociation,[4,11–13] Radio frequency (RF) discharge,[14] and direct current (DC) pulsed discharge.[7,15,16] The emission spectrum is a conventional and convenient spectroscopy technology capable of offering valuable information about studied atoms or molecules.[15,17–23] Electronically excited CH ($A^2\Delta$) produced by the multi-photon dissociation has been investigated.[4,24–26] Lichtin *et al*. observed electronically excited CH through the photodissociation of $CHBr_3$ at 266 nm and proposed the mechanism of a three-photon process.[4] Chen *et al*. further proposed a three-step sequential bromine atom elimination mechanism for the photodissociation of $CHBr_3$ at 266 nm.[24] Jörg *et al*. also proposed the dissociation channels for the production of CH ($A^2\Delta$) by the multi-step photodissociation of $CHBr_3$ using ArF and KrF excimer lasers.[25] Chikan *et al*. investigated the process of the dissociation of bromoform through two different means: a 266-nm femtosecond laser and synchrotron radiation.[17] They concluded that the primary channel of the multiphoton dissociation of $CHBr_3$ at 266 nm is a sequential break of three C–Br bonds. Butler *et al*. photodissociated CH_3NO_2 at 193 nm and figured out that the primary process is the cleavage of the C–N bond to yield CH_3 and NO_2.[26] Takashi Nagata *et al*. observed the unequal intensities of the Λ-doublet components in the CH ($A^2\Delta - X^2\Pi$) emission following the multiphoton dissociation of $(CH_3)_2CO$, $(CH_3)_2S$, and CH_3NO_2 by an ArF laser (193 nm).[27] Also, Yang *et al*. investigated the multiphoton dissociation mechanisms of bromomethanes ($CHBr_3$, $CHBr_2Cl$, $CHBrCl_2$, and CH_2Br_2) at 266 nm using both the nascent emission spectrum and the laser-induced dispersed fluorescence spectrum.[28] As far as we know, till now there has been no report about the study of the CH radical produced by photodissociation using the fifth harmonic of the YAG laser at $\sim$ 213 nm.

In this paper, we investigate the production of CH radicals by photodissociating four different samples [$(CH_3)_2CO$, CH_3NO_2, CH_2Br_2, and $CHBr_3$]. The rest of this paper is arranged as follows. In Section 2, we give our schematic diagram of the experimental setup and a brief introduction. In Section 3, we present our experimental results about CH production by the photodissociation of the above-mentioned precusors using the fifth harmonic of the YAG laser, and compare their relative signal intensities by the CH ($A \rightarrow X$) emission spectrum under the same experimental conditions. We study the power dependences of the multi-photon dissociation for the samples mentioned above, except $(CH_3)_2CO$. We also study the relationship between the signal intensity and some

*Project supported by the National Natural Science Foundation of China (Grant Nos. 10674047, 10804031, 10904037, 10904060, 10974055, 11034002, 11274114, and 61205198), the National Key Basic Research and Development Program of China (Grant Nos. 2006CB921604 and 2011CB921602), and the Basic Key Program of Shanghai Municipality, China (Grant No. 07JC14017), the Fundamental Research Funds for the Central Universities, and the Shanghai Leading Academic Discipline Project, China (Grant No. B408).

†Corresponding author. E-mail: jpyin@phy.ecnu.edu.cn

© 2014 Chinese Physical Society and IOP Publishing Ltd

parameters, such as the temperature of the beam source, the stagnation pressure, and the delay between the opening of the valve and the photolysis laser. The influences of three different carrier gases on the signal intensity are further investigated. The vibrational and rotational temperatures of the CH product are obtained by comparing experimental data with the simulated ones from the LIFBASE program. In Section 4, we summarize the main results and give a conclusion.

2. Experimental section

The schematic diagram of the experimental setup is illustrated in Fig. 1. Our chamber consists of two parts: a source chamber and a science one. The present work of CH production reported here is performed in the source chamber. Further scientific research on CH radicals will be performed in the science chamber later. The source chamber and science one are each pumped by a 1200-l/s turbo molecular pump (KYKY, FD-1200K). An inert carrier gas (He, Ar, Kr) at the 3 atm (1 atm = 1.01325×10^5 Pa) stagnation pressure is bubbled through the samples ($(CH_3)_2CO$, CH_3NO_2, CH_2Br_2, and $CHBr_3$) in a stainless steel reservoir and then adiabatically expands through a solenoid valve (General Valve, Series 9, ϕ0.2 mm) into a vacuum. During operation, the pressure in the source chamber is typically 2×10^{-3} Pa. The transistor–transistor logic (TTL) trigger signals generated by a five-channel digital delay/pulse generator (Model GH024) are sequentially sent to the pulse valve, Boxcar (Model SR250, Stanford), 200-MHz digital oscilloscope (Agilent Technology), and the fifth harmonic of the YAG laser (QUANTEL-Brilliant B) at $\sim$ 213 nm. The laser beam is focused by a lens with a focal length of 30 cm. The fluorescence generated by the excited CH product sequentially passes through a convex lens, a mirror, and another convex lens before it enters into the entrance slit of a monochromator (BEIJIN 7-STAR OPTICAL INSTRUMENTS CO., LTD; MODE:71SW 301). An effective slit width of 10 μm and a 1200-lines/mm grating make the monochromator reach a resolution of 0.1 nm. The light output from the monochromator is collected by a photomultiplier tube (PMT) (BEIJIN 7-STAR OPTICAL INSTRUMENTS CO., LTD; MODE: 71D101-CR131). The electric signal of the PMT output is transferred to a boxcar. The signal processed by the boxcar then enters into a data acquisition system (BEIJIN 7-STAR OPTICAL INSTRUMENTS CO., LTD; MODE: 71DA1) controlled by the computer. The emission spectrum of CH($A\rightarrow X$) is obtained by scanning the monochromator. The samples used in the experiment are $(CH_3)_2CO$ (analytically pure, Sinopharm Chemical Reagent Co., Lid), CH_3NO_2 (chemically pure, Sinopharm Chemical Reagent Co., Lid), $CHBr_3$ (analytically pure, Sinopharm Chemical Reagent Co., Lid), and CH_2Br_2 (chemically pure, Sinopharm Chemical Reagent Co., Lid). The carrier gases used are He ($\geq$ 99.999%, Shanghai Five Steel Gas Co. Ltd.), Ar ($\geq$ 99.999%, Shanghai Five Steel Gas Co. Ltd.), are Kr (PRAXAIR, INC. East Chicago, Indiana), and the power meter used is from Newport with the 1918-C model.

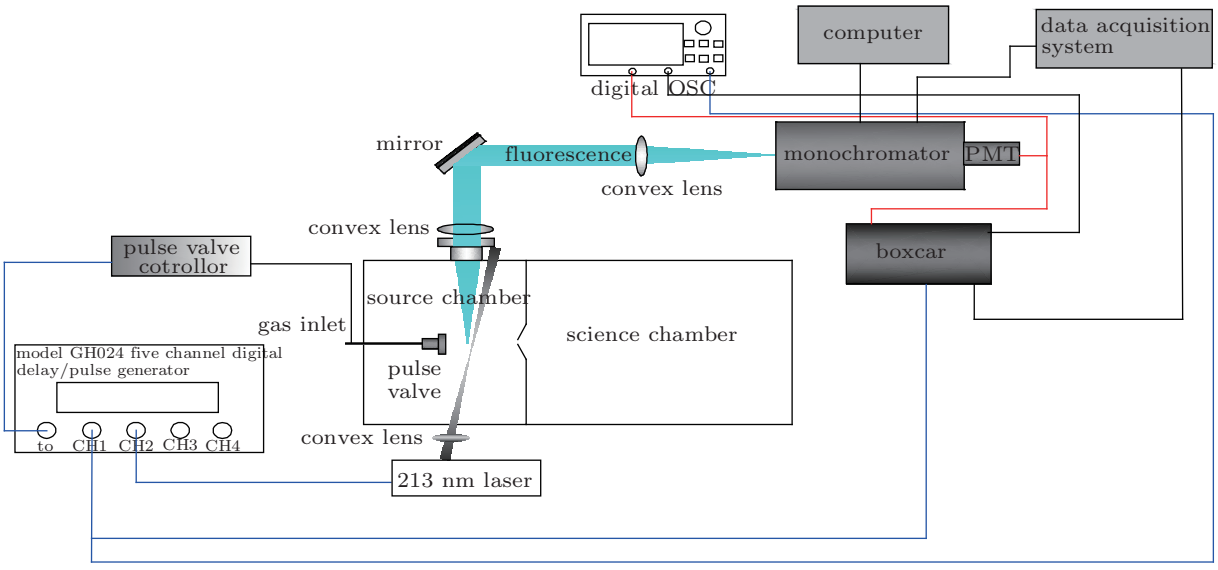


Fig. 1. (color online) Schematic diagram of experimental setup.

3. Results and discussion

3.1. CH ($A\rightarrow X$) emission spectrum

We observe the emission spectra of CH radical ($A\rightarrow X$) by dissociating four different samples ($(CH_3)_2CO$, CH_3NO_2, CH_2Br_2, and $CHBr_3$) using the $\sim$ 213-nm laser. The CH ($A\rightarrow X$) emission spectra of the four different samples are measured under almost the same conditions. The parameters used for the experiments are as follows: stagnation pressure is

3 atm, the energy of the laser pulse is kept at 8 mJ, the voltage applied on the PMT is −900 V, and the pulse valve is opened for 170 μs. As we can see from Fig. 2, the intensity of the CH radical is weakest when $(CH_3)_2CO$ is chosen as the parent molecule. In the work by Takashi *et al.*,[27] $(CH_3)_2CO$ is almost the same as CH_3NO_2 in terms of efficiency as a precursor for CH production at ∼ 193 nm. The reason lies in the fact that absorption cross sections of $(CH_3)_2CO$ are different at different wavelengths. At a temperature of 294 K, the absorption cross sections of $(CH_3)_2CO$ are 1.318×10^{-21} cm^2 and 3.13×10^{-18} cm^2 for the ∼ 213 nm and ∼ 193 nm, respectively. While the absorption cross sections of CH_3NO_2 are of nearly the same order of magnitude for the ∼ 213 nm and ∼ 193 nm. The absorption cross sections at ∼ 213 nm of the other three samples (CH_3NO_2, CH_2Br_2, and $CHBr_3$) are 1.296×10^{-17} cm^2, 2.548×10^{-18} cm^2, and 4.58×10^{-18} cm^2, respectively. The saturated vapor pressures at 294 K for the four samples ($(CH_3)_2CO$, CH_3NO_2, CH_2Br_2, and $CHBr_3$) are 24.64 kPa, 3.71 kPa, 4.65 kPa, and 665 Pa, respectively. The above-mentioned two factors together with the photon number absorbed for dissociation and the quantum yield into the product channel of interest here account for the differences in the signal intensity of CH radicals from four precursors, which will be discussed further later.

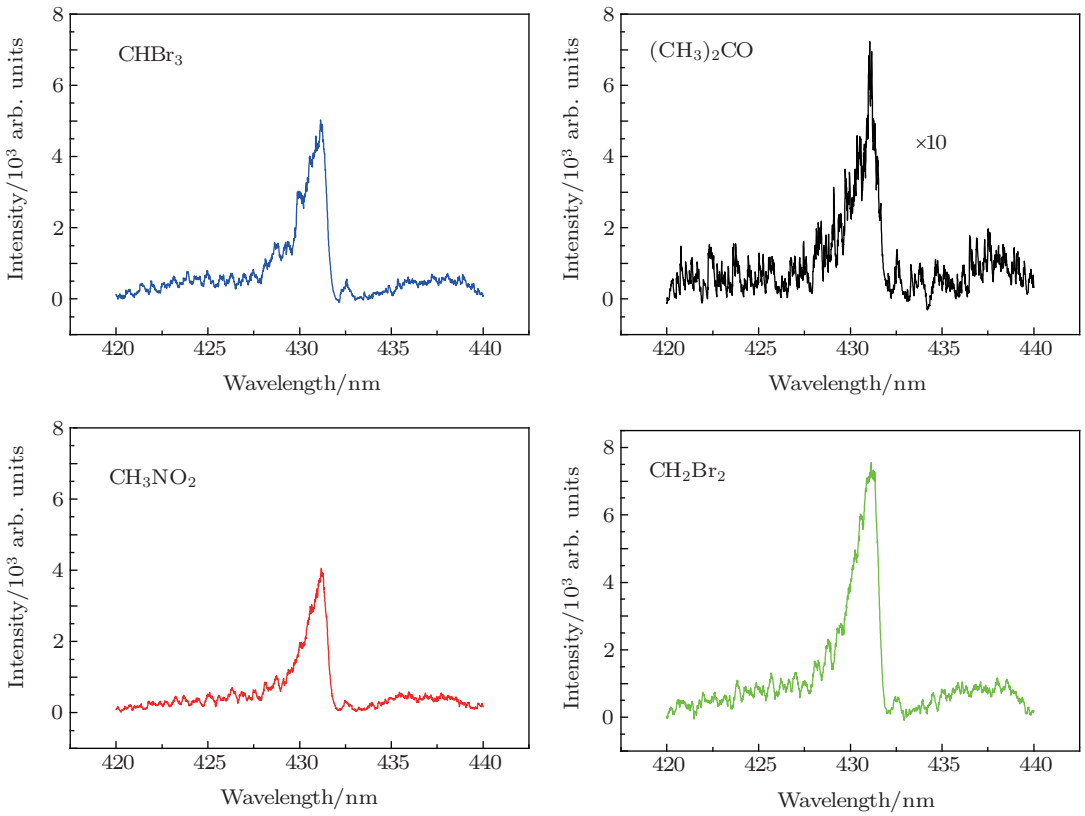


Fig. 2. (color online) The CH ($A \rightarrow X$) emission spectra produced by the ∼ 213-nm laser photodissociation of the four different samples ($(CH_3)_2CO$, CH_3NO_2, CH_2Br_2, and $CHBr_3$).

3.2. Power dependence of the multi-photon dissociation

The power dependence of the total $A \rightarrow X$ emission of the CH product is recorded by changing the pulse energy of the ∼ 213-nm laser for the samples mentioned above except $(CH_3)_2CO$, which has a rather weak signal and a poor signal-to-noise ratio.

Figure 3(a) shows the power dependence in a double logarithmic plot of the CH signal from the photodissociation of $CHBr_3$ at ∼ 213 nm. Here the signal intensity is obtained by integrating the emission spectrum of the CH radical. From the slope, the order of the multi-photon dissociation process is determined to be 1.8, so at least two photons are needed in the multi-photon dissociation process. Chikan *et al.*[17] listed the energetically possible processes from the photodissociation of bromoform. Considering the energy needed in these dissociation channels, the most likely dissociation channel for our experiment is $CHBr_3 \rightarrow CH(A) + Br + Br_2(X)$, which requires a total energy of about ∼ 9.89 eV lower than the total energy of two ∼ 213-nm photons of ∼ 11.67 eV. Other channels require an energy higher than that provided by two ∼ 213-nm photons.

When CH_2Br_2 is chosen as a parent molecule, at least three photons are involved in the multi-photon dissociation process, as shown in Fig. 3(b). In his doctoral thesis,[29] Chim listed some possible dissociation channels, such as $CH(A^2\Delta) + HBr + Br$, $CH(A^2\Delta) + H + Br_2$,

$CH(A^2\Delta) + H + 2Br$, with the energies needed being 9.91 eV, 11.23 eV, and 13.67 eV, respectively. Considering the three photons involved in the process of photodissociation, we infer that the probable channel is $CH(A^2\Delta) + H + 2Br$.

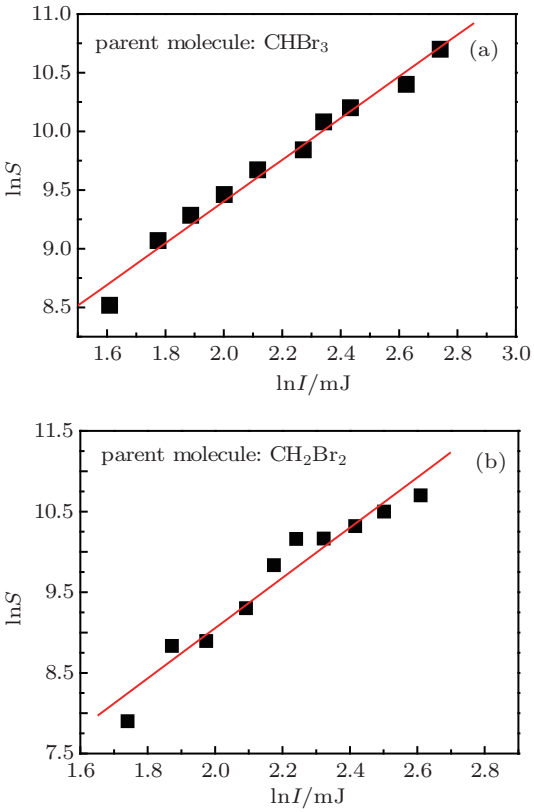


Fig. 3. (color online) Plots of the intensity of the CH emission spectrum versus photolysis laser power (213 nm) on a natural log scale. The samples used are (a) $CHBr_3$ and (b) CH_2Br_2.

For CH_3NO_2 as a parent molecule, the slope order of the multi-photon dissociation process is determined to be 2.8, so at least three photons are needed in the multi-photon dissociation process. The plot is similar to that in Fig. 3(b) and not given here to save space. As confirmed by several groups,[30–34] the main primary process of nitromethane photolysis is the cleavage of the C–N bond. We suppose that the process of nitromethane dissociation is as follows: first, the break of the C–N bond, $CH_3NO_2 + h\upsilon \rightarrow CH_3 + NO_2$, followed by a sequential two-step hydrogen atom elimination process with CH_3 and CH_2 radicals as intermediate products.

3.3. Signal intensity dependence on other parameters

3.3.1. Temperature of the source

Here we take $CHBr_3$ as an example. The sample is kept in a stainless steel reservoir. An electro-thermostatic water bath is used to heat the reservoir and keep its temperature constant. The temperature can be varied from 20 °C to 90 °C. As shown in Fig. 4(a), the higher the temperature, the larger the signal intensity is. The saturated vapor pressure of $CHBr_3$ turns higher as the temperature increases. This plot gives only a rough trend rather than a quantitative scenario of the temperature dependence, since the sample temperature inside the pulse valve is hard to know accurately.

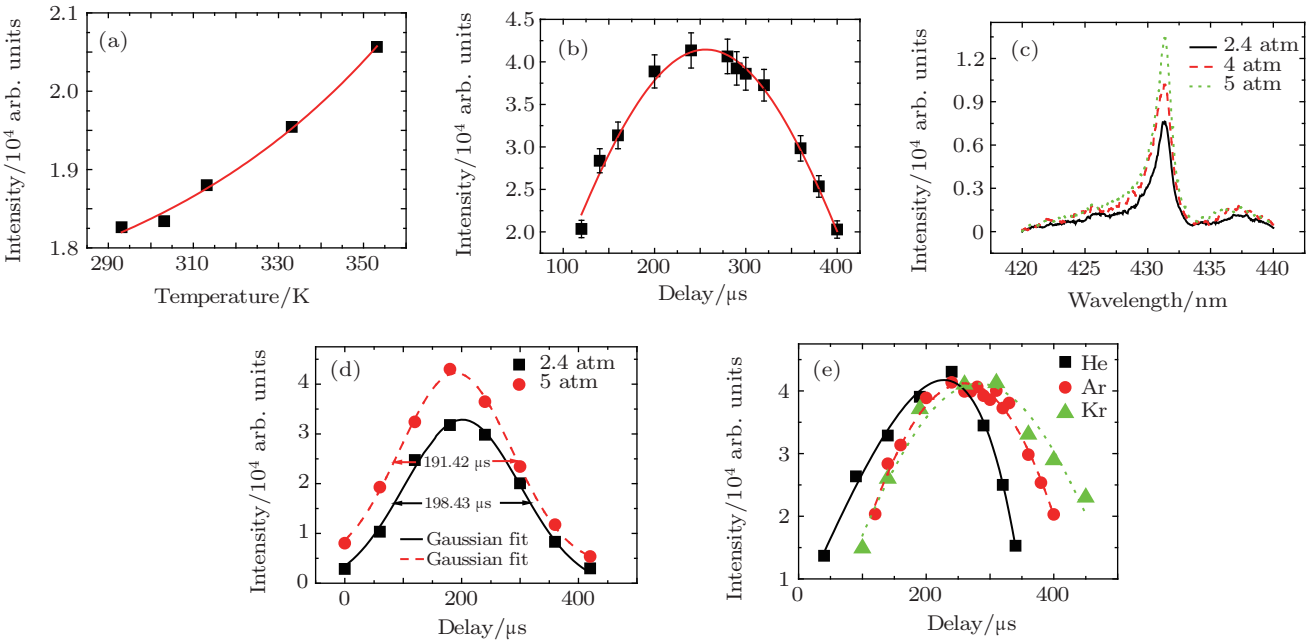


Fig. 4. (color online) Factors influencing the intensity of the CH ($A \rightarrow X$) emission spectrum: (a) the temperature of the source, (b) the time delay between the pulse valve and the laser, and (c) the stagnation pressure of the source. (d) The comparison between the signal intensity and the delay time under two different stagnation pressures of the source. (e) The influence of the carrier on the signal intensity for three kinds of carriers.

3.3.2. Time delay between the pulse valve and the laser

The right time delay is critical for seeing the signal of CH in the experiment. Here we take $CHBr_3$ and argon as the parent molecule and carrier gas. As the delay grows, the signal intensity first increases, then decreases and has its maximum near the value of ~ 250 μs, as shown in Fig. 4(b). This time delay dependence is a reflection of the velocity distribution of the precursors in the longitudinal direction.

3.3.3. Stagnation pressure of the source

Here we take CH_3NO_2 as the parent molecule. The delay between the laser and the valve is ~ 240 μs, the voltage applied to the PMT is -900 V, the temperature is about ~ 20 °C, and the pulse energy of the laser is about 9 mJ. As shown in Fig. 4(c), the black solid line, red dash line, and the green dot line show the cases with source stagnation pressures of ~ 2.4 atm, ~ 4.0 atm, and ~ 5.0 atm, respectively. As we can see, the higher the stagnation pressure, the stronger the signal is. To better understand this, we further study the relationships between the signal intensity and the time delay under two different pressures. As shown in Fig. 4(d), the black (solid square) points and the red (solid circle) points are experimental data for source stagnation pressures of ~ 2.4 atm and ~ 5.0 atm, respectively. The black (solid) line and red (solid) line are the corresponding Gaussian fittings. We can see that the signal intensity under ~ 5.0 atm is consistently larger than that under ~ 2.4 atm, especially for a time delay near 240 μs. The full width at half maximum (FWHM) of the Gaussian fittings for ~ 2.4 atm and ~ 5.0 atm are 198.43 μs and 191.42 μs, respectively. From the FWHM of the Gaussian fittings, we can infer that the longitudinal velocity distribution at ~ 5.0 atm is narrower than that at ~ 2.4 atm. The explanation is as follows: a higher source pressure results in a larger precursor number density in the laser dissociation region, and thus yielding more CH products. Huo and Qu[35] studied the relationship between the beam intensity and the source pressure, and gave a theoretical formula as follows:

$$I = \frac{p}{4kT}\sqrt{\frac{8kT}{m\pi}}S,$$

where I is the beam intensity, p is the source pressure, and S is the area of the orifice. In his book *Atomic and Molecular Beam Methods*, Giacinto Scoles[36] presented a similar conclusion that the beam intensity increases with the increasing of the source pressure. In addition, the higher the source pressure, the better the adiabatic expansion of the supersonic beam will be, which will result in a narrower longitudinal velocity distribution of the supersonic beam and a lower longitudinal temperature.

3.3.4. Influence of the carrier gas

For studying what role the carrier gas plays, helium, argon, and krypton are used in the experiment. As shown in Fig. 4(e), black solid squares, red solid circles, and green solid triangles denote the data points for cases with helium, argon, and krypton respectively, with solid lines being the corresponding fitting lines. The comparison clearly shows that the carrier gas mainly affects the optimal time delay between the pulse valve and the laser. The optimal delay gradually increases from helium to krypton due to the decrease in beam velocity after supersonic expansion. Reference [15] shows that a worse signal-to-noise ratio is obtained when argon is used as a carrier gas instead of helium, and many extra lines arise from atomic and discharge products if a DC pulse discharge is used for CH production. In discharge, the energy for breaking the C–Br bond is provided by the metastable atoms (He^*, Ar^*), excited from collisions with high-energy electrons. Metastable Ar is much lower in energy than metastable He.[30] This accounts for the low efficiency of CH ($A^2\Delta$) production when argon is used as a carrier gas. Unlike the case of discharge, in the process of photodissociation, we observe no such extra lines arising from atomic products since there appear to be no metastable atoms and the energy for breaking the C–Br bond is obtained directly from the photon. This is why the efficiency for CH ($A^2\Delta$) production is almost unchanged when different carrier gases are used.

3.4. Vibrational and rotational temperatures

Due to the limited resolution of the monochromator (1200 lines, 500 nm), the rotational spectrum cannot be distinguished clearly. We analyze the vibrational and rotational temperatures of the CH products by comparing the experimental data with the simulation results from the LIFBASE program.[37] Figure 5 shows the temperatures of the CH product with CH_2Br_2 serving as a precursor, the red dash curve and the black solid curve are the experimental and simulated results, respectively. For the vibrational and rotational temperatures of ~ 3300 K and ~ 3300 K respectively, the simulated data fit to the experimental one well (Peak correlation: 0.997117, Chi-square: 9.4638). Chikan *et al.* dissociated bromoform using a synchrotron radiation and a 266-nm femtosecond laser[17] separately. They calculated the rotational temperatures of CH ($A^2\Delta$) through the Boltzmann distribution of the intensity of the rotational lines and obtained the results of $T^{\rm rot}_{v'=0} = 3650 \pm 150$ K (synchrotron radiation) and $T^{\rm rot}_{v'=0} = 4250 \pm 300$ K (266-nm femtosecond laser). The vibrational and rotational temperatures can also be evaluated via comparing the experimental data with the simulated results from the commercial programs, like LIFBASE. Wang *et al.*[38] produced the CH ($A^2\Delta$) radical using the DC pulse discharge and obtained the vibrational and rotational temperatures of $T_{\rm vib} = 4575$ K and $T_{\rm rot} = 2455$ K, respectively. The vibrational and rotational temperatures of

our produced CH ($A^2\Delta$) from the precursor of CH_2Br_2 are in general accordance with the results of other groups. We do not attempt to make a direct comparison between results of each group since different experimental conditions are used.

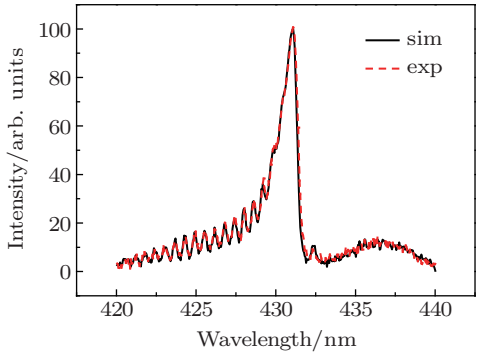


Fig. 5. (color online) Vibrational and rotational temperatures obtained through the comparison between the experimental (exp) data and the simulation (sim) results provided by the LIFBASE program.

4. Conclusions

In this paper, we studied the preparation of the CH product by the photodissociation of several samples ($(CH_3)_2CO$, CH_3NO_2, CH_2Br_2, and $CHBr_3$) through using the fifth harmonic of the YAG laser at $\sim$ 213 nm. The signal intensities of the CH product from different precursors were compared by observing the CH ($A \rightarrow X$) emission spectra under almost the same experimental conditions, and found that the intensity of the CH signal produced by the photodissociation of acetone is about seven times weaker than that of nitromethane at $\sim$ 213 nm, unlike the results obtained at $\sim$ 193 nm. The power dependences of the multi-photon dissociation for the above precursors except $(CH_3)_2CO$ were examined. The orders of the multi-photon dissociation process at $\sim$ 213 nm were measured to be 2, 3, and 3 for $CHBr_3$, CH_3NO_2, and CH_2Br_2, respectively. We also investigated the factors affecting the signal intensity, such as the temperature of the source, the time delay between the opening of the pulse valve and the laser, the stagnation pressure of the source, and carrier gas species, and figure out that the carrier gases play different roles in the DC pulse discharge and the photodissociation. The vibrational and rotational temperatures of the CH ($A^2\Delta$) product were obtained by comparing the experimental data with the simulated ones from the LIFBASE program. For instance, with CH_2Br_2 serving as a precursor, the CH product has vibrational and rotational temperatures of $\sim$ 3300 K and $\sim$ 3300 K respectively. Due to its large ratio between the dipole moment and mass, the prepared CH molecule can be used to realize electrostatic Stark deceleration,[39] accurate measurement,[9] cold collisions and cold chemistry,[40,41] and so on.

References

[1] Heurlinger T 1918 Ph. D. thesis, University of Lund
[2] Heurlinger T and Hulthen E 1919 *Z. Wiss. Photogr. Photophys. Photochem.* **18** 241
[3] Kind M, Stuhi F, Tzeng Y R, Alexander M H and Dagdigian P J 2001 *J. Chem. Phys.* **114** 4479
[4] Lichtin D A, Bermun M R and Lin M C 1984 *Chem. Phys. Lett.* **108** 18
[5] Nishiyama N, Sekiya H, Yamaguchi S, Tsuji M and Nishimura Y 1986 *J. Phys. Chem.* **90** 1491
[6] Dean A J, Hanson R K and Bowman C 1991 *J. Phys. Chem.* **95** 3180
[7] Takezaki M, Ohoyama H, Kasai T and Kuwata K 1994 *Laser Chem.* **15** 113
[8] Ikejiri K, Ohoyama H, Nagamachi Y and Kasai T 2005 *Chem. Phys. Lett.* **401** 465
[9] Truppe S, Hendricks R J, Tokunaga S K, Lewandowski H J, Kozlov M J, Christian Henkel, Hinds E A and Tarbutt M R 2013 *Nat. Commun.* **4** 2600
[10] Nagamachi Y, Ohoyama H, Yamakawa K and Kasai T 2006 *Chem. Phys. Lett.* **421** 124
[11] Fotakis C, Martin M and Donovan R J 1982 *J. Chem. Soc. Faraday Trans.* **2,78** 1363
[12] Zou P, Shu J N, Sears T J, Hall G E and North S W 2004 *J. Phys .Chem. A* **108** 1482
[13] Baronavski A P and Mcdonald J R 1978 *Chem. Phys. Lett.* **56** 369
[14] Avtaeva S V, Mamytbekov M Z and Otorbaev D K 1997 *J. Phys. D: Appl. Phys.* **30** 3000
[15] Romanzin C, Boye-Peronne S and Gauyacq D, Benilan Y, Gazeau M C and Douin S 2006 *J. Chem. Phys.* **125** 114312
[16] Anderson D T, Davis S, Zwier T S and Nesbitt D J 1996 *Chem. Phys. Lett.* **258** 207
[17] Chikan V, Fournier F and Leone S R 2006 *J. Phys. Chem. A* **110** 2850
[18] Zhang L, Yang J M and Jin F T 2011 *Acta Phys. Sin.* **60** 045210 (in Chinese)
[19] Zhou Q C 2006 *Acta Phys. Sin.* **55** 4618 (in Chinese)
[20] Zhang S D and Li H Y 2003 *Acta Phys. Sin.* **52** 1297 (in Chinese)
[21] Feng J, Wang J S, Gao Y F and Zhan M S 2001 *Acta Phys. Sin.* **50** 1279 (in Chinese)
[22] Guo H and Tang P 2009 *Chin. Phys. B* **18** 3457
[23] Guo H and Tang P 2013 *Chin. Phys. B* **22** 054204
[24] Chen C X, Ran Q, Yu S Q and Ma X X 1993 *Chem. Phys. Lett.* **203** 307
[25] Lindner J, Ermisch K and Wilhelm R 1998 *Chem. Phys.* **238** 329
[26] Butler L J, Krajnovich D and Lee Y T 1983 *J. Chem. Phys.* **79** 1708
[27] Nagata T, Suzuki M, Suzuki M, Kondow T and Kuchitsu K 1984 *Chem. Phys.* **88** 163
[28] Yang S X, Hou G Y, Dai J H, Chang C H and Chang B C 2010 *J. Phys. Chem. A* **114** 4785
[29] Chim R Y L 2003 Ph. D. thesis, University of Birmingham
[30] Rebbet R E and Slagg N 1962 *Bull. Soc. Chim. Belges.* **71** 709
[31] Gray P, Yoffe A and Roselaar D 1955 *L. Trans. Faraday Soc.* **51** 1489
[32] Nicholson A J C 1961 *Nature* **190** 143
[33] Avouris P, Chan I Y and Loy M M T 1980 *J. Photochem.* **13** 13
[34] Rockney B H and Grant E R 1981 *Chem. Phys. Lett.* **79** 15
[35] Huo B H and Qu J T 1999 *College Phys.* **18** 38 (in Chinese)
[36] Scoles G 1988 *Atomic and Molecular Beam Methods* (New York: Oxford Press) pp. 33–35
[37] "LIFBASE: Database and Spectral Simulation for Diatomic Molecules", ed. Luque J and Coquart D R, Merienne M F and Simon P C 1989 *Planet. Space Sci.* **37** 1127
[38] Wang X M, Yang S D, Chen Y Q and Yang X H 2006 *Acta Opt. Sin.* **26** 1866
[39] Fu G B, Deng L Z and Yin J P 2008 *Chin. Phys. Lett.* **25** 923
[40] Krems R V 2008 *Phys. Chem. Chem. Phys.* **10** 4079
[41] Loison J C and Bergeat A 2009 *Phys. Chem. Chem. Phys.* **11** 655